

# Thermo-elastic response of the Juno spacecraft's solar array/magnetometer boom

M. Herceg<sup>1</sup>, P.S. Joergensen<sup>1</sup>, J. L. Joergensen<sup>1</sup>, J. E. P. Connerney<sup>2,3</sup>

<sup>1</sup>Technical University of Denmark (DTU), Lyngby, Denmark (mher@space.dtu.dk)

<sup>2</sup>Space Research Corporation, Annapolis, MD, United States

<sup>3</sup>NASA Goddard Space Flight Center, Greenbelt, MD, United States

Corresponding author: Matija Herceg (mher@space.dtu.dk)

## Abstract

Juno was inserted into a highly elliptic, polar, orbit about Jupiter on July 4<sup>th</sup> 2016. Juno's magnetic field investigation acquires vector measurements of the Jovian magnetic field using a flux gate magnetometer co-located with attitude-sensing star cameras on an optical bench. The optical bench is placed on a boom at the outer extremity of one of Juno's three solar arrays. The Magnetic Field investigation (MAG) uses measurements of the optical bench inertial attitude provided by the micro Advanced Stellar Compass ( $\mu$ ASC) to render accurate vector measurements of the planetary magnetic field. During periJoves, MAG orientation is determined using the spacecraft (SC) attitude combined with transformations between SC and MAG. Substantial pre-launch efforts were expended to maximize the thermal and mechanical stability of the Juno solar arrays and MAG boom. Nevertheless, flight experience demonstrated that the transformation between SC and MAG reference frames varied significantly in response to spacecraft thermal excursions associated with large attitude maneuvers and proximate encounters with Jupiter. This response is monitored by comparing attitudes provided by the MAG investigation's four CHU's and the spacecraft attitude. These attitude disturbances are caused by the thermo-elastic flexure of the Juno solar array in response to temperature excursions associated with maneuvers and heating during close passages of Jupiter. In this paper, we investigate these thermal effects and propose a model for compensation of the MAG boom flexure effect.

## 34 **1 Introduction**

35 As a fully autonomous star tracker, the MAG's micro Advanced Stellar Compass ( $\mu$ ASC)  
 36 services the Juno MAG attitude determination requirement by comparison of the star field with a  
 37 matching star field stored in an on-board star catalog (Connerney et al., 2017). Juno's MAG  
 38 boom is a four-meter extension at the outer extremity of one of Juno's three solar panel arrays.  
 39 Juno is a spin-stabilized spacecraft rotating nominally at 2 rotations per minute (rpm) about the z  
 40 axis which is closely aligned with the spacecraft telecommunications antenna. To optimize the  
 41 attitude determination function on a spinning spacecraft, the four  $\mu$ ASC star cameras (CHUs) are  
 42 oriented on the Juno spacecraft with an angular separation of  $13^\circ$  between optical and spin axes.  
 43 The CHUs have an optical field of view (FOV) of  $13^\circ$  by  $18^\circ$  and scan the sky continuously in  
 44 the anti-sunward direction, imaging every 0.25 seconds and producing attitude quaternions at  
 45 that rate (though telemetry allocations dictate downlink cadence).

46 The MAG investigation was planned with several pathways to provide attitude determination for  
 47 the fluxgate sensors (Connerney et al., 2017), and that flexibility proved useful when Juno's  
 48 mission plan transitioned, after orbit insertion, from one with 14-day orbits to one with 53-day  
 49 orbits (Bolton et al., 2017). To acquire the same number (34) of orbits provided for in the  
 50 original mission plan, Juno would be required to operate over a much broader range of local  
 51 times than it was designed for. As a result, during most periJoves, the ASC CHUs would  
 52 encounter Jupiter in the FOV for at least some of the time, preventing continuous attitude  
 53 determination throughout the critical periJove passage. As a result, the MAG investigation  
 54 elected a backup attitude determination strategy in which attitudes are derived from the  
 55 spacecraft attitude solution (c-kernel) using a transformation between the MAG optical bench  
 56 and the spacecraft determined by comparison (when available) between the ASC CHUs and the  
 57 spacecraft SRU.

58 Direct comparison of the spacecraft attitude solutions with those provided by the CHUs on the  
 59 MAG boom revealed a systematic variation in the attitude of the MAG Boom as Juno transited  
 60 the solar system during cruise, attributed to mechanical deformation of the solar array as it  
 61 cooled while moving further from the sun (Connerney et al., 2017). Once Juno arrived on orbit, a  
 62 similar deformation was observed during periJove passes, attributed to heating of the solar array  
 63 by Jupiter. We note that the MAG boom itself proved to be remarkably stable, throughout cruise  
 64 and during orbital operations, but as it is affixed to the outer end of the solar array, a distortion of  
 65 the array perturbs the attitude of the MAG Boom. The solar array bends in response to the  
 66 increase in temperature due to non-isotropic coefficient of thermal expansion (CTE) related to  
 67 the design of the mechanical assemblage. The array substrate can be thought of as a sandwich  
 68 consisting of thin carbon-composite face sheets encasing an aluminum honeycomb core (typical  
 69 of lightweight spacecraft construction). By itself it would likely be fairly benign in its thermal

response, but one side (sunward facing) is coated with silicon cells and cover glass, with a CTE unlike that of the substrate.

The increase in temperature associated with a periJove passage is measured by multiple thermal sensors on the solar array and is just a few degrees C (about 5 or 6 degrees for most periJoves) from a typical baseline temperature of about -130° C. However, that is sufficient to alter the boom (and MAG sensor) attitude by almost 0.1°. This thermal distortion is brief in duration (~2 hours) and the array returns to its pre-periJove attitude after thermal relaxation, but the distortion occurs at the time of highest scientific interest. An attitude determination error of this magnitude would compromise the vector accuracy of the magnetic field measurement (in strong magnetic fields) if not corrected for. Since Juno periapsis passages are just above the planet's cloudtops, and Jupiter has a very strong planetary magnetic field (Connerney et al., 2018), every passage transits a strong magnetic field magnitude (~4 to ~16 G).

Identification of the thermal distortion of the solar array necessitated implementation of a time dependent transformation between spacecraft and MOB. The objective of this study is to characterize the thermal distortion of the mechanical appendage, determine its dependence on array temperature, and offer a model whereby the attitude disturbance can be predicted with confidence and removed from the data. This report also serves to bring awareness to subtle effects that may limit measurement accuracy on flight systems that do not benefit from sensors capable of monitoring mechanical stability.

## 2 Modeling of the thermo-elastic effects

The relevant Juno reference frames, and the transformations between them, are presented in Fig 1.  $M_{SC}$  is the transformation matrix describing the Juno spacecraft orientation in the inertial (J2000) reference frame, extracted from NAIF c-kernels, and  $M_{CHU}$  is the transformation matrix describing the orientation of a CHU in the inertial (J2000) frame, determined from  $\mu$ ASC measurements. Fixed transformations between the Juno SC and each of the 4 ASC CHU's ( $Juno\_CHU\#\_TO\_SC$ ), as defined in the NAIF frame (FK) kernel file, may be represented via sequential rotations about the spacecraft x, y, and z axes (Table 1).

	Rot3 Z	Rot3 Y	Rot3 X
S/C->CHU A	178.950	1.370	-167.035
S/C->CHU B	179.125	1.150	167.035
S/C->CHU C	-1.000	0.480	-166.480
S/C->CHU D	-0.220	0.510	167.380

**Table 1: Fixed transformations between the Juno SC and each of the 4 ASC CHU's, represented via sequential rotations about the spacecraft x, y, and z axes**

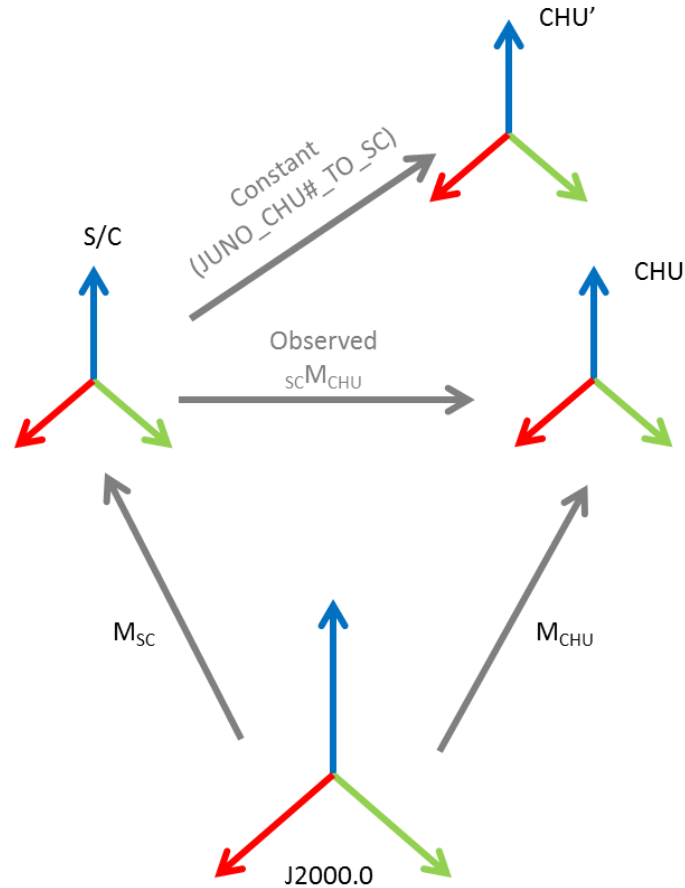


**Figure 1: Coordinate frames utilized for the thermo-elastic boom model and relations between them.**

The transformation from the SC frame to that of the InBoard (IB) or OutBoard (OB) MOBs (see Fig 2) was originally envisioned as a static transformation that might change from one periJove to another, perhaps in response to infrequent spacecraft propulsive maneuvers, but was assumed to remain unchanged throughout a periJove pass. The MAG boom itself proved to be remarkably stable over environmental conditions, as determined by inter-comparison of the four CHUs. Each MOB contains a pair of CHUs, mounted to the MOB with kinematic mounts (as are the fluxgate sensors) which have proven remarkably stable. The MAG boom itself is a large (~4m) 3-dimensional structure constructed of aluminum honeycomb, carbon-composite faced, with longitudinal stiffeners running the length of the structure, fully enclosed in multi-layer thermal insulating blankets.

The MAG investigation anticipated the need to verify in flight the deployment attitude of the MAG boom, and periodically monitor the relationship between spacecraft attitude and MOB attitude, and as a result a series of attitude calibration exercises were scheduled before and after

major propulsive maneuvers (Connerney et al., 2017). We learned that while propulsive maneuvers resulted in transient disturbances, the MAG boom attitude returned very close to pre-maneuver orientation. However, when comparing the spacecraft attitude solution during periJove passages with attitudes measured each 0.24 s by the CHUs, we observed a systematic variation quickly identified as a response of the Juno solar array to the increase in temperature due to Jupiter thermal emission. Thus the need for a predictive model resulting in a time-dependent transformation between spacecraft and MOB.

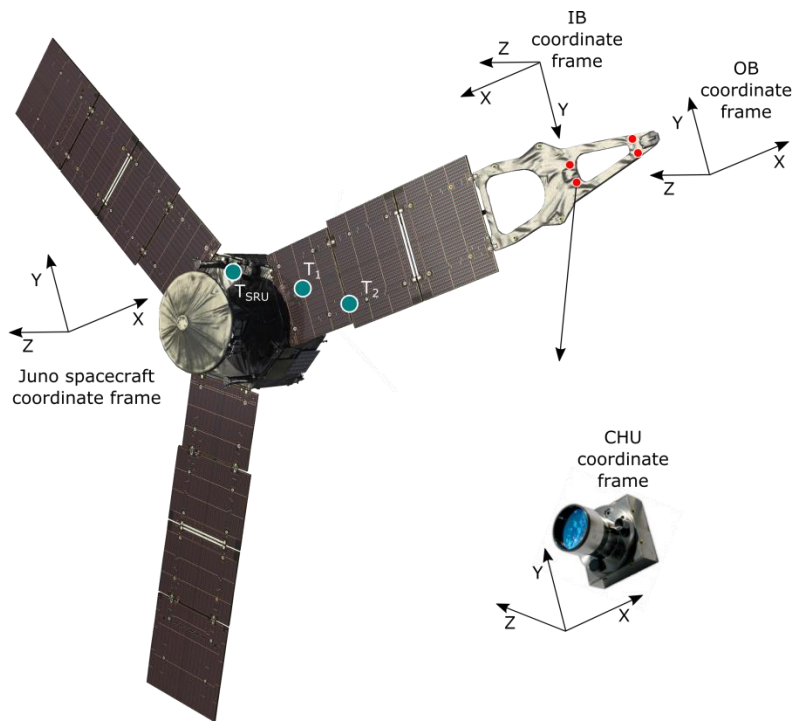


**Figure 2: The Juno spacecraft, the  $\mu$ ASC CHU and the MAG instrument coordinate frames. Turquoise circles show locations of the Wing 1 solar array thermistors ( $T_1$  and  $T_2$ ) and Stellar Reference Unit thermistors ( $T_{SRU}$ ). Red circles show locations of the four  $\mu$ ASC CHU's. Rotation about the y-axis of the SC is where bending of the Juno wing 1 is observed.**

Comparison of the CHU attitude observations and SC orientation in the CHU reference frame ( ${}_{sc}M_{chu}$ ) shows a systematic variation with periJove passage, remarkably consistent from one periJove passage to the next (Fig 3) with one exception having to do with spacecraft attitude during periJove passage. Most orbits in the Juno mission plan are executed with the spacecraft

spin axis, and telecom antenna, directed toward Earth for gravity science (Bolton et al., 2017). On occasion, periJoves are executed with the spin axis directed off Earth-point in a manner that optimizes passage of the microwave radiometer (MWR) field of view (and that of other instruments) as it scans across the planet. These two kinds of orbits – called ‘GRAV’ and ‘MWR’ orbits for short – lead to different thermal responses most easily identified by the attitude of the Mag boom upon approach to periJove and the disturbance in attitude ~6 hours after periJove as the spacecraft re-acquires Earth pointed attitude.

Transformation between the SC and CHU frame is ( ${}_{sc}M_{chu}$ ) is defined as:

$${}_{sc}M_{chu}=M_{CHU} \cdot M_{SC}^T \quad (1)$$

Comparison of the Juno CHU and SC orientation in the CHU reference frame is calculated by applying the preflight fixed transformations between the two frames:

$${}_{sc}M_{chu\_REL}=M_{Juno\_CHU\#\_TO\_SC} \cdot {}_{sc}M_{chu}^T \quad (2)$$

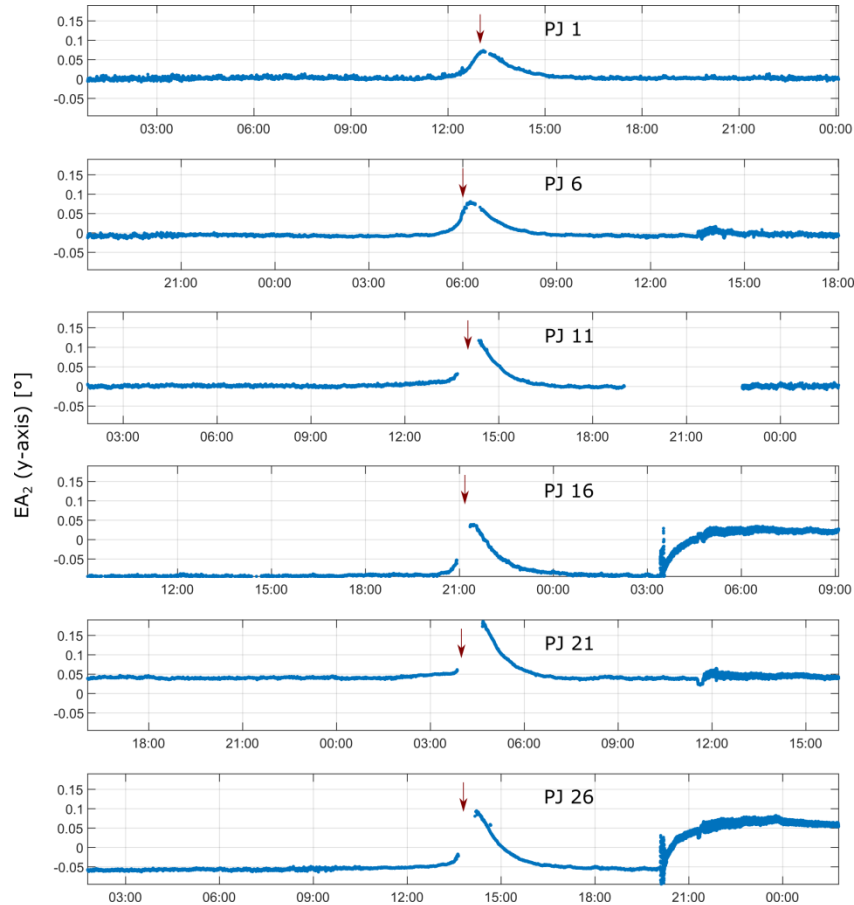


**Figure 3: Comparison of the Juno CHU B and SC orientation expressed as a rotation about the spacecraft y-axis in the CHU reference frame (for the PJ 1, 6, 11, 16, 21 and 26). A fixed rotation (bias) about y-axis of  $1.15^\circ$  has been removed. PJs 16 and 26 illustrate MWR orbits, in which the spacecraft approaches Jupiter off Earth-point, and returns to Earth pointed attitude  $\sim 6$  hours post-PJ. Red arrows indicate the time of the periJove.**

The Juno spacecraft is equipped with a multitude of thermal sensors to monitor temperatures throughout the spacecraft, including several deployed along the solar array (wing #1) hosting the MAG boom. Two of these ( $T_1$  and  $T_2$  in Figure 2) have proven very useful in modeling the array response, as illustrated in Figure 4. Comparison of the temperature and attitude variation shows a clear correlation between the disturbance rotation angle about the CHU B y-axis and the solar array temperature (bottom two panels, Figure 4).

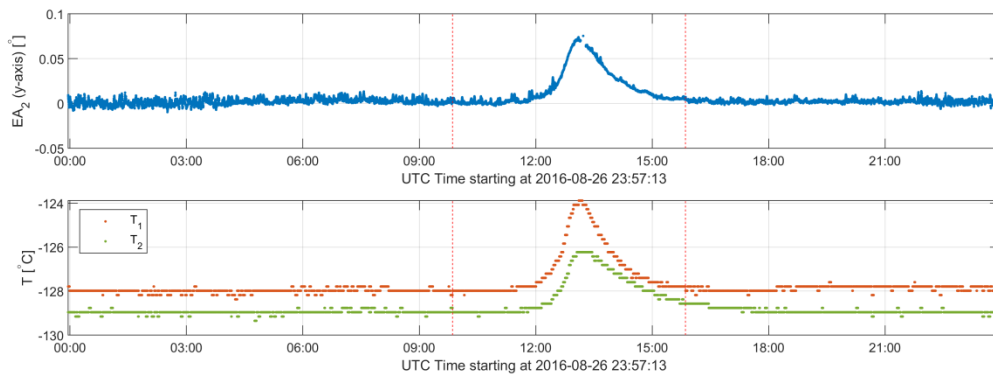


**Figure 4: Juno SC rotation about the y-axis in the CHU B reference frame for PJ 1 (top plot), Juno wing 1 solar panel thermistor observations ( $T_1$  and  $T_2$ , second plot)**

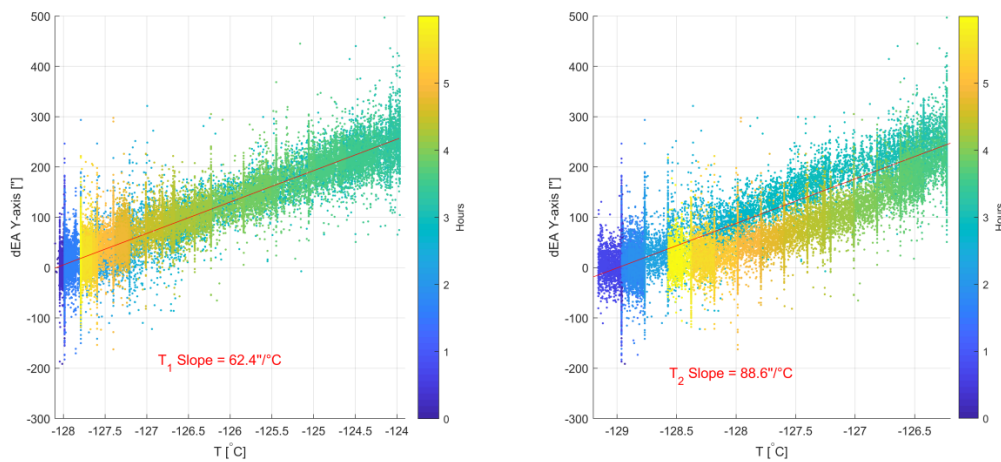


**Figure 5: Correlation between the rotation about the y-axis variation and Juno solar panel temperatures ( $T_1$  and  $T_2$ ). Correlation is shown for the period +/- 3 hours around the periJove**

For the purpose of correcting the relative orientation between the SC and each CHU for thermal effects, a thermal compensation model was defined using valid attitude data from the very first periJove (PJ 1). A model was constructed using the orientation of each CHU with respect to the SC orientation in the camera frame combined with Juno wing 1 solar panel temperatures  $T_1$  and  $T_2$ .  $T_1$  is a compact reference for Lockheed Martin's (LM) engineering telemetry channel T-0237 SA1pan1Temp, and  $T_2$  refers to LM's T-0446 SA1pan2Temp, output from Juno's wing 1 solar panel thermistors. In addition to the solar panel temperatures,  $T_1$  and  $T_2$ , the model uses Stellar Reference Unit (SRU) thermistors to compensate for the small quasi-periodic attitude perturbations visible on the x-axis. These relatively minor attitude errors (in the spacecraft c-kernel attitude estimation) are caused by the slight thermal distortion of the mechanical structure supporting the SRU. These perturbations correlate well with a combination of the outputs from the two thermistors associated with this subsystem; the SRU is heated by two independently-controlled heaters cycling on and off in a quasi-periodic manner. We use the SRU-based temperature proxy  $T_{SRU}$  that is the mean of the SRU temperatures ( $T_{SRU} = (SRU1_{Temp1} + SRU2_{Temp1})/2$ ).

To estimate the parameters of the thermal model (rotations) based on the observed temperatures and frames differences, a Singular Value Decomposition (SVD) of the linear system of equations was used. The resulting thermal model describes how each transformation between CHU and SC changes due to the observed temperature of the Juno wing 1 structure and it is defined as:

$$M_{Juno\_CHU\#\_TO\_SC\_CORR} = R_1(\alpha) \cdot R_2(\beta) \cdot R_1(\gamma) \cdot M_{Juno\_CHU\#\_TO\_SC} \quad (3)$$

Where each rotation is described by:

$$R_1(\alpha) = \begin{bmatrix} 1 & 0 & 0 \\ 0 & \cos(\alpha) & \sin(\alpha) \\ 0 & -\sin(\alpha) & \cos(\alpha) \end{bmatrix} \quad (4)$$

$$R_2(\beta) = \begin{bmatrix} \cos(\beta) & 0 & -\sin(\beta) \\ 0 & 1 & 0 \\ \sin(\beta) & 0 & \cos(\beta) \end{bmatrix} \quad (5)$$



$$R_3(\gamma) = \begin{bmatrix} \cos(\gamma) & \sin(\gamma) & 0 \\ -\sin(\gamma) & \cos(\gamma) & 0 \\ 0 & 0 & 1 \end{bmatrix} \quad (6)$$

And individual rotation angles are represented as follows:

$$\alpha = \alpha_0 + \alpha_1 T_1 + \alpha_2 T_2 + \alpha_3 T_{SRU} \quad (7)$$

$$\beta = \beta_0 + \beta_1 T_1 + \beta_2 T_2 + \beta_3 T_{SRU} \quad (8)$$

Model derived from the SVD is shown in Table 1.

Resulting thermal model coefficients derived from SVD is shown in *Table 2*.

CHU A				
	$\alpha$	$\beta$	$\gamma$	
<b>Constant</b>	0.0836	-2.3869	-0.3924	[°]
<b>T<sub>1</sub></b>	0.0019	-0.0140	-0.0028	[°/°C]
<b>T<sub>2</sub></b>	-0.0011	-0.0045	6.0e-05	[°/°C]
<b>T<sub>SRU</sub></b>	-0.0009	-8.0e-05	-0.0019	[°/°C]
CHU B				
	$\alpha$	$\beta$	$\gamma$	
<b>Constant</b>	0.0673	-2.1642	0.4530	[°]
<b>T<sub>1</sub></b>	0.0013	-0.0131	0.0022	[°/°C]
<b>T<sub>2</sub></b>	-0.0006	-0.0036	0.0016	[°/°C]
<b>T<sub>SRU</sub></b>	-0.0010	-0.0009	-0.0022	[°/°C]
CHU C				
	$\alpha$	$\beta$	$\gamma$	
<b>Constant</b>	-0.0764	2.3342	-0.5756	[°]
<b>T<sub>1</sub></b>	-0.0021	0.0138	-0.0042	[°/°C]
<b>T<sub>2</sub></b>	0.0013	0.0043	-1.0e-05	[°/°C]
<b>T<sub>SRU</sub></b>	0.0009	5e-05	-0.0018	[°/°C]
CHU D				
	$\alpha$	$\beta$	$\gamma$	
<b>Constant</b>	-0.0374	2.3487	0.4798	[°]
<b>T<sub>1</sub></b>	-0.0017	0.0135	0.0039	[°/°C]

$T_2$		0.0013	0.0046	0.0001		$[\text{°/°C}]$
$T_{\text{SRU}}$		0.0009	0.0008	-0.0017		$[\text{°/°C}]$

**Table 2: Thermal model coefficients based on PJ 1 (2016-240) for transformation between Juno SC and each of the  $\mu$ ASC CHU's.**

As seen from the model coefficient table, the angular deviation is almost entirely a rotation about the spacecraft y-axis ( $\beta$ ), which is parallel to the solar array hinge line; this is consistent with the attitude variation observed during cruise (Connerney et al., 2017) in response to the secular cooling of the array in transit from Earth to Jupiter, during which a rotation of  $\sim 1^\circ$  of rotation about spacecraft y axis was observed. It is also the rotation expected of bending due to unmatched CTE on sunward-facing and dark sides of the solar array.

### 3 Results

In Figure 6 we show a comparison of the CHU and spacecraft attitudes as measured using a fixed transformation with that using a variable transformation based on the thermal model output. The corrected attitudes show significant improvements. The thermal model completely removes the variation caused by the bending of the boom (rotation about the y axis) and shows virtually no residual variation apart from white noise. Likewise, the quasi-periodic attitude errors appearing as rotations about the x and z axis are removed well using the SRU temperature proxy. The root mean square residual attitude error (RMS) of rotation about the y-axis, after correction, is 8 arc-seconds, compared to 72.1 arc-seconds found using the uncorrected (static) transformation.

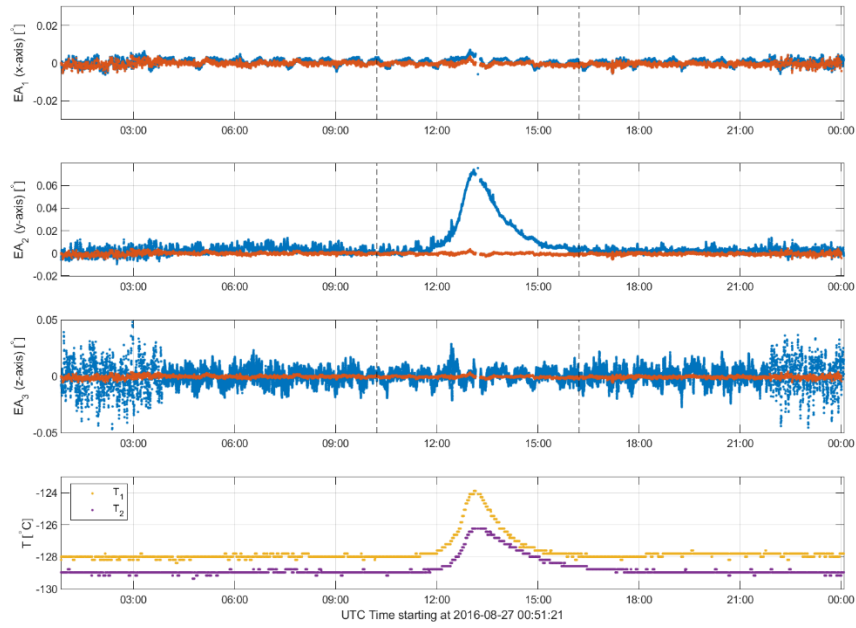


**Figure 6: Relative comparison of the Juno CHU B and SC orientation in the CHU B reference frame (PJ1, 2016-240). Top three panels: Blue shows uncorrected deflection angles. Red shows deflection angles after correction and applying a 60 seconds moving average. Bottom panel: Shows the two SC solar panel temperatures.**

It is important to mention that modeling was based only on the data from the PJ1 (2016-240). Application of the model outside of the modeling period (for the PJ3 to PJ27 dataset) shows similarly good results, as seen in the example illustrated in Fig 7 for periJove 26. By applying the model to the PJ26 data, RMS of the rotation error about the y-axis is reduced from 129.0 to 8.5 arc-seconds. This is a very impressive result, considering the date we correct for is almost 4 years after the model was computed and that the range of thermal distortion is twice the range of that used to establish the model parameters.

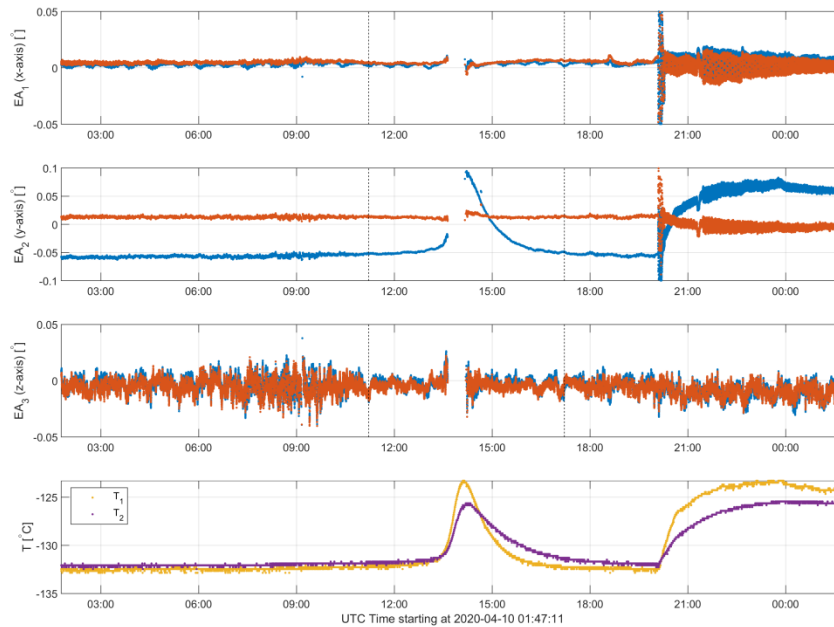


**Figure 7: Relative comparison of the Juno CHU B and SC orientation in the CHU B reference frame (PJ26, 2020-101). Top three panels: Blue shows uncorrected deflection angles. Red shows deflection angles after correction and applying a 60 seconds moving average. Bottom panel: Shows the two SC solar panel temperatures.**

Fig 7 illustrates the model efficacy as applied to an MWR orbit, in which the spacecraft attitude is altered well in advance of the periJove pass (so that the spacecraft attitude perturbations are well damped). As a result, the solar array is a bit further off sun as well, and the spacecraft enters the periJove interval represented here off Earth point, and therefore somewhat cooler than normal (GRAV orbit). This effect is also well modeled and the corrected attitude is brought back to nearly 0 degrees for the periJove. The rapid re-orientation about 6 hours post-PJ is somewhat less well corrected and evidences a long lasting disturbance that slowly yields to the spacecraft fluid nutation dampers.

As demonstrated, the choice of the proxy temperatures and model parameters estimated with the SVD solution provide excellent compensation of the thermal disturbances. The results after applying thermal model show virtually no variation of relative orientation between SC and CHU's, apart from noise and settling effects of the Earth-point precession. Note that modeling period was based solely on the PJ1 data (2016-240), and the model has been applied on data well beyond the modelling period and thermal range, up to PJ26. Using the model coefficients, a NAIF c-kernels is computed for each MOB using a thermo-elastic model (Table 1) of the boom

deflection as a function of temperature. These thermo-elastic MOB c-kernels have been provided to NAIF for archive along with the spacecraft c-kernels.

Performance of the proposed model for the compensation of Juno wing thermo-elastic instability for periJoves 1-27 can be found in the supplementary material to this paper. Attention to mechanical stability is but one consideration in the measurement accuracy achieved on a flight platform. Juno is the first spacecraft to venture beyond Earth orbit with a magnetic field investigation suitably endowed with sensors to track attitude stability of the magnetometer boom (necessitated by the need to separate spacecraft and magnetic sensors). Juno's very accurate vector magnetic field measurements also revealed the presence of relatively small spacecraft fields generated within the conductive MAG boom structure itself as the spacecraft slowly spins (2 rpm) in the presence of a strong magnetic field (Eddy current generation). Correction for this effect was described by Kotsiaros et al. (2020) who presented a finite element model of Eddy current generation in the vicinity of the MAG sensors. This effort and the thermal modeling described here illustrate the need for a comprehensive systems approach in achieving high accuracy measurements on space platforms.

**Acknowledgements:** We thank the project and support staff at the Jet Propulsion Laboratory (JPL), Lockheed Martin, and the Southwest Research Institute (SWRI) for the design, implementation, and operation of the Juno spacecraft. We are particularly indebted to Lockheed Martin mechanical engineer, Russ Gehring, who was responsible for the design and fabrication of the MAG boom. JPL manages the Juno mission for the principal Investigator, S. Bolton, of SWRI. This research is supported by the Juno Project under NASA grant NNM06AAa75c to SWRI, and NASA grant NNN12AA01C to JPL/Caltech. The Juno mission is part of the New Frontiers Program managed at NASA's Marshall Space Flight Center in Huntsville, Alabama. The authors are aware of no real or perceived conflicts of interest with respect to the results of this paper. All data used in this article is available in the main text and in the supplementary materials, as well as in the permanent archival data repository, Zenodo (Herceg et al, 2020).

## References

- Bolton, S.J., Lunine, J., Stevenson, D. *et al.* The Juno Mission. *Space Sci Rev* **213**, 5–37 (2017). <https://doi.org/10.1007/s11214-017-0429-6>
- Connerney, J.E.P., Benn, M., Bjarno, J.B. *et al.* The Juno Magnetic Field Investigation. *Space Sci Rev* **213**, 39–138 (2017). <https://doi.org/10.1007/s11214-017-0334-z>
- Connerney, J.E.P., Lawton, P., Kotsiaros, S., Herceg, M. The Juno Magnetometer (MAG) Standard Product Data Record and Archive Volume Software Interface Specification (SIS)

302 Herceg, M., Jørgensen, P.S., Jørgensen, J. L. Characterization and compensation of thermo-  
303 elastic instability of SWARM optical bench on micro Advanced Stellar Compass attitude  
304 observations, *Acta Astronautica*, Volume 137, August 2017, Pages 205-213.  
305 <https://doi.org/10.1016/j.actaastro.2017.04.018>

306 Kotsiaros, S., Connerney, J. E. P., and Martos, Y. (2020). Analysis of Eddy current generation on  
307 the Juno spacecraft in Jupiter's magnetosphere, *Earth and Space Science*,  
308 doi:10.1029/2019EA001061

309 Herceg, M., Jørgensen, P.S., Jørgensen, J. L., J.E. Connerney: Supplementary material for *Thermo-*  
310 *elastic response of the Juno spacecraft's solar array/magnetometer boom*, Zenodo DOI:  
311 10.5281/zenodo.3936080

312

313

314